Research Article

Comprehensive understanding on sources of high levels of fine particulate nitro-aromatic compounds at a coastal rural area in northern China

Yueru Jiang[1], Xinfeng Wang[1,*], Min Li[1], Yiheng Liang[1,2,3], Zhiyi Liu[1], Jing Chen[1], Tianyi Guan[1], Jiangshan Mu[1], Yujiao Zhu[1], He Meng[4], Yang Zhou[5], Lan Yao[6], Likun Xue[1], Wenxing Wang[1]

[1] Environment Research Institute, Shandong University, Qingdao 266237, China

[2] Department of Environmental Systems Science, Swiss Federal Institute of Technology Zurich, Zurich 8092, Switzerland

[3] Department of Water Resources and Drinking Water, Swiss Federal Institute of Aquatic Science and Technology, Duebendorf 8600, Switzerland

[4] Qingdao Eco-Environment Monitoring Center of Shandong Province, Qingdao 266003, China

[5] College of Oceanic and Atmospheric Sciences, Ocean University of China, Qingdao 266100, China

[6] School of Environmental and Geographical Sciences, Shanghai Normal University, Shanghai 200234, China

ARTICLE INFO

ABSTRACT

Nitro-aromatic compounds (NACs) are among the major components of brown carbon (BrC) in the atmosphere, causing negative impacts on regional climate, air quality, and ecological health. Due to the extensive origins, it is still a challenge to figure out the contributions and originating regions for different sources of atmospheric NACs. Here, field observations on fine particulate NACs were conducted at a coastal rural area in Qingdao, China in the winter of 2018 and 2019. The mean total concentrations of fine particulate nitro-aromatic compounds were 125.0 ± 89.5 and 27.7 ± 21.1 ng/m^3 in the winter of 2018 and 2019, respectively. Among the measured eleven NACs, nitrophenols and nitrocatechols were the most abundant species. Variation characteristics and correlation analysis showed that humidity and anthropogenic primary emissions had significant influences on the NAC abundances. In this study, two tracing methods of the improved spatial concentration weighted trajectory (SCWT) model and the receptor model of positive matrix factorization (PMF) were combined to comprehensively understand the origins of NACs in fine particles at coastal Qingdao. Four major sources were identified, including coal combustion, biomass burning, vehicle exhaust, and secondary formation. Surprisingly, coal combustion was responsible for about half of the observed nitro-aromatic compounds, followed by biomass burning ($\sim$30%). The results

* Corresponding author.
  E-mail: xinfengwang@sdu.edu.cn (X. Wang).

by SCWT demonstrated that the coal combustion dominated NACs mainly originated from the Shandong peninsula and the areas to the north and southwest, while those dominated by biomass burning primarily came from local Qingdao and the areas to the west.

1.   Introduction

Nitro-aromatic compounds (NACs), with the nitro (-NO$_2$) and hydroxyl (-OH) substituted groups are directly linked to an aromatic ring, have been characterized as important constituents of brown carbon (BrC) due to the light-absorbing properties at near-UV light (Yang et al., 2022). Field studies showed that they were responsible for around 4% of the BrC light absorption at 370 nm in the United Kindom and Los Angeles while as high as 17% in Beijing (Li et al., 2020b; Mohr et al., 2013; Zhang et al., 2013). Furthermore, the photolysis of NACs in the region of 300–500 nm contributes to the formation of nitrous acid (HONO) and hydroxyl radicals (-OH), which further has an effect on atmospheric chemistry processes and secondary pollutant formation (Bejan et al., 2006; Cheng et al., 2009; Wang et al., 2020). NACs not only affect regional climate and air quality, but also have adverse impacts on human health and plant growth. It has been recognized that they are toxic and carcinogenic and are to a certain degree responsible for forest decline in North Europe (Harrison et al., 2005; Kovacic and Somanathan, 2014). Particularly, NACs can react with hemoglobin to reduce the ability of cells to deliver oxygen to tissues and organs, leading to blood disorders (Agency for Toxic Substances and Disease Registry, 2015). Owing to the strong effects on the earth atmosphere and the ecological environment, NACs have gained growing attentions in the recent years.

The abundances of fine particulate NACs vary with locations and seasons, changing from below one to several hundred ng/m^3. Numerous field observations have been conducted in rural, urban, suburban, as well as background sites around the world. The observed concentrations of NACs at urban sites are usually higher than other types of sites, as a result of the dense anthropogenic activities in the urban regions (Morville et al., 2006; Teich et al., 2017; Wang et al., 2018). In addition, their contents in winter are substantially higher than in summer (Chow et al., 2015; Kahnt et al., 2013; Li et al., 2020a; Wang et al., 2018), partly associated with the intensive combustion activities for heating and facilitated gas-particle partitioning under low temperature conditions (Bidleman, 1988; Li et al., 2020a). Among the various NAC species, 4-nitrophenol and 4-nitrocatechol are commonly the most abundant components due to their extensive origins, abundant precursors, high emission factors, and relatively long atmospheric lifetime (Yuan et al., 2021). Nevertheless, nitro-salicylic acids can be the most abundant species in remote areas in summer owing to the enhanced photochemical formation processes (Teich et al., 2017; Wang et al., 2018). Overall, the large variations of NACs in the abundance and compositions in different atmospheric environments reflect their complex and diverse origination.

The atmospheric NACs originate from a large number of anthropogenic emission sources such as coal combustion (Lu et al., 2019b; Lüttke et al., 1997), biomass burning (Hoffmann et al., 2007; Iinuma et al., 2010; Wang et al., 2017), vehicle exhaust (Lu et al., 2019a; Tremp et al., 1993), and industries activities such as production and usage of pesticides (Delhomme et al., 2010; Harrison et al., 2005; Lu et al., 2021), as well as the secondary formation via oxidation reactions of aromatic compounds in the presence of nitrogen oxides (Harrison et al., 2005). In addition, it is also proposed that aqueous-phase oxidation of precursors acts as extra formation pathway for some NACs, *e.g.*, nitrosalicylic acids can be formed from aqueous-phase salicylic acid nitration in the presence of N$_2$O$_5$ or HNO$_3$ (Andreozzi et al., 2006; Chen et al., 2021; Harrison et al., 2005; Liang et al., 2020). Furthermore, aqueous-phase oxidation is considered to be the major formation pathway for methyl-nitrocatechols under high NO$_x$ in Beijing (Wang et al., 2019). The contributions of different sources to the atmospheric NACs have been successfully estimated by receptor model such as Positive Matric Factor (PMF). Gu et al. (2022) found that atmospheric NACs were mainly from secondary formation and traffic emissions during foggy days in suburban Nanjing. Ren et al. (2022) reported that the sources of NACs were dominated by coal combustion and biomass burning in spring and by secondary formation in summer in urban Beijing. Yuan et al. (2021) demonstrated that coal combustion and biomass burning were the major contributors of NACs in winter in Xi'an, whereas in summer, secondary formation and vehicle emissions contributed the most part. Li et al. (2020a) suggested that coal combustion was the predominant contributor to the wintertime NACs in urban Jinan and secondary formation had a large contribution in summer, while vehicle exhaust was recognized as the main source in spring. In addition, the PMF-derived results indicated that secondary formation and aged coal combustion served as the major sources of NACs in the summer at the summit of Mt. Tai and rural sites in Yucheng and Wangdu in Wang et al. (2018). The source identification and quantification provide an important basis for pollution mitigation of atmospheric NACs. However, to achieve accurate pollution control, it is essential to further recognize their main source regions. In previous studies, concentration weighted trajectory (CWT) method has been widely employed to identify potential source regions for atmospheric pollutants (Cheng et al., 2013; Feng et al., 2021; Wong et al., 2022). Nevertheless, with consideration of the fact that the concentration changes when the air mass pass through different heights and locations, there can be some bias in the traditional CWT method with treating the concentration the same for all points along the air mass trajectory. Therefore, improved method by considering the discrepant influence on the concentrations in different spatial locations
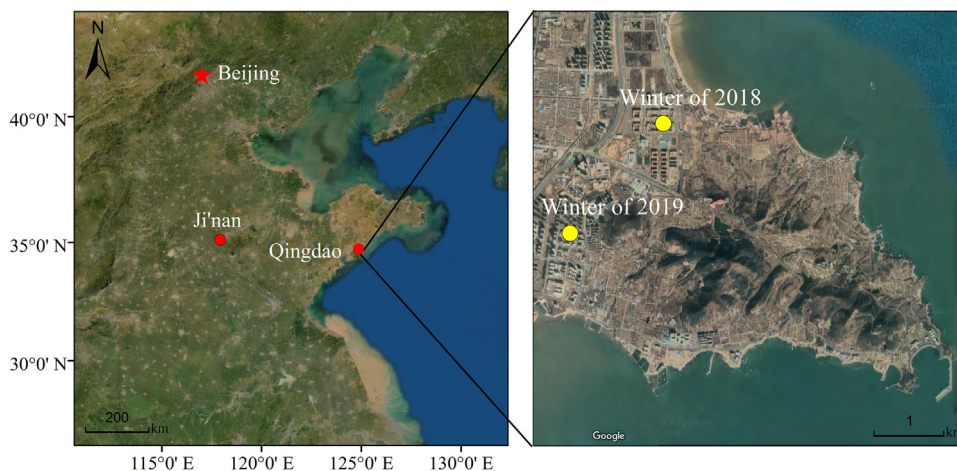
Fig. 1 – Maps showing the location of the observation sites in Qingdao

is required to obtain reliable understanding on the potential source regions.

In the present study, fine particulate matter samples were collected at a coastal rural area in Qingdao in cold seasons and high levels of NACs were observed. The temporal variation characteristics and the influencing factors were then analyzed. Finally, the major sources and the main originating regions were identified with the combination of the PMF receptor model and the improved spatial concentration weighted trajectory (SCWT) model.

2. Experiments and methods

2.1. Sampling sites

The field sampling and online measurements were conducted at two adjacent rural sites in the winter of 2018 and 2019 in Qingdao, a coastal city in northern China (Fig. 1). The two sites are close to each other with a linear distance of ~2.2 km. They are close to the Yellow Sea. There is a national express way to the west and some education areas, residential districts, and villages scatter nearby. More detailed information about the sampling sites and their features were described by Liu et al. (2022).

2.2. Sample collection and online measurements

In total, 140 atmospheric fine particulate matter (PM$_{2.5}$) samples were collected on 88-mm quartz filters (Pall, USA) by using a TH-150A medium-volume sampler (100 L min^{-1}, Wuhan Tianhong). The field sampling was conducted during the winter of 2018 (January 10 – February 23 2019) and the winter of 2019 (November 11 – December 25 2019). Two samples were acquired per day during daytime (8:00–19:30, local time) and nighttime (20:00–7:30). In addition to the PM$_{2.5}$ samples, five field blanks were also obtained at the beginning and the end of the filed campaigns with the pump not running. Before sample collection, the quartz filters were baked in a muffle at 550°C for 3 hr to preclude potentially adsorbed organic substances.

Before and after sampling, all filters were equilibrated for 48 h at constant temperature of 20 ± 5°C and constant humidity of 50% ± 2% and then were weighed with a Sartorius ME5-F electronic microbalance. Once the sample collection finished, the filter samples were stored at -20 °C in the dark until subsequent chemical analysis.

In the winter of 2018, the levels of trace gases including ozone (O$_3$), sulfur dioxide (SO$_2$), nitrogen oxide (NO$_x$ = NO + NO$_2$), and carbon monoxide (CO) were monitored in real time by commercial gas analyzers by utilizing photometric detection methods (Thermo Scientific, USA). The hourly data of meteorological variables covering ambient temperature (T), relatively humidity (RH), wind direction, and wind speed were obtained from the Weather Underground (https://www.wunderground.com, last access: 25 January 2022). At the same time, the mass concentrations of PM$_{2.5}$ were obtained from a nearby air quality monitoring station of Yangkou. In the winter of 2019, the data of trace gases, PM$_{2.5}$, and meteorological parameters were achieved from the adjacent newly-built ambient air quality monitoring station (Liu et al., 2022).

2.3. Sample extraction and chemical analyses

A section of filter (30 cm^2) was cut into small pieces and ultrasonically extracted three times with 15 ml of high purity methanol (HPLC grade, Sigma-Aldrich) for 30 min. The extracted solutions were combined together and then concentrated to near dry with a rotary evaporator. The residuals were re-dissolved in 2 ml methanol and subsequently filtered through a polytetrafluoroethylene syringe filter (0.22 μm pore size, Millex-FG). The filtrate was enriched under high-purity nitrogen stream. The dried samples were finally re-dissolved in 300 μL methanol which contains 200 ppb 2,4,6-trinitrophenol as the internal standard.

An ultra-high-performance liquid chromatograph (UHPLC-MS) coupled with an ISQ EC mass spectrometer (Ultimate 3000, Thermo Scientific) was used to measure the nitro-aromatic compounds in sample solutions. Electrospray ionization (ESI) source was operated under selective negative ion mode. The target substances were separated by an At-

lantis T3 C18 column (2.1 μm particle size, 2.1 mm × 150 mm, Waters, USA). The column was operated at 30°C with an injection volume of 10 μL. The mobile phase comprised methanol with 11% acetonitrile (eluent A) and deionized water with 11% acetonitrile and 0.1% formic acid (eluent B) and worked at a flow rate of 0.2 ml min^{-1}. The gradient elution procedure was as follows: the fraction of A was set as 34% in the beginning and gradually rose to 66% within 19 min. It was then hold for 4 min at 66% and finally decreased to 34% within 8 min. Target analytes were identified by comparing the retention time and mass spectra with those of the authentic standards. Eleven NACs were identified from PM$_{2.5}$ samples in this study, i.e. 4-nitrocatechol (4NC), 3-methyl-6-nitrocatechol (3M6NC), 4-methyl-5-nitrocatechol (4M5NC), 4-nitrophenol (4NP), 3-methyl-4-nitrophenol (3M4NP), 2-methyl-4-nitrophenol (2M4NP), 2,6-dimethyl-4-nitrophenol (2,6DM4NP), 2,4-dinitrophenol (2,4DNP), 4-methyl-2,6-dinitrophenol (4M2,6DNP), 5-nitrosalicylic-acid (5NSA), 3-nitrosalicylic-acid (3NSA). They were quantified with multi-point calibration curves ($r^2 > 0.99$). The recovery rates of the analytes were obtained by spiking standard solutions on blank filters by following the same method mentioned above, in the range of 68–96%. Note that the recovery rates via ultrasonic extraction were compared with those via oscillatory extraction. The extraction efficiencies by ultrasonication were substantially better than osicillation and no apparent interference was found, so ultrasonic extraction was selected in this study. The chemicals used in this study were purchased from Sigma-Aldrich (St. Louis, MO, USA), J&K Chemical (Beijing, China), and Atomax Chemicals (Shenzhen, China).

In addition, a 2 cm^2 punch of sample filter was cut to analyze the concentrations of organic carbon (OC) and elemental carbon (EC) with a carbon aerosol analyzer (Sunset, Model 3, USA) by thermal-optical method according to the protocol of NIOSOH. The content of organic matter (OM) was calculated as 1.59 times the OC concentration according to a previous study in Qingdao in winter (Xing et al., 2013).

2.4. Receipt source apportionment model

Positive matrix factorization (PMF) model, a multi-factor analysis technique, has been extensively employed to determine and to quantify the specific sources of ambient pollutants (Li et al., 2022; Reizer et al., 2021; Song et al., 2021b; Yuan et al., 2021; Zhang et al., 2022). In the present study, we applied the U.S. Environmental Protection Agency PMF 5.0 software to identify the major sources and to evaluate their contributions to fine particulate NACs. The files input to the PMF model includes concentration data and uncertainty data (see Eq. (1)). The uncertainties for each species were calculated as follows (Brown et al., 2015; Luo et al., 2022).

$$Unc = \begin{cases} 5/6 \times MDL & C_{ij} \leq MDL \\ \sqrt{\left(0.1 \times C_{ij}\right)^2 + \left(0.5 \times MDL\right)^2} & C_{ij} > MDL \end{cases} \quad (1)$$

where, C_{ij} is the concentration of the species i in the sample j, and MDL is the method detection limit for each species.

A dataset consisting of 10 species including nine NACs of 4NP, 3M4NP, 2M4NP, 2,6DM4NP, 4NC, 4M5NC, 3M6NC, 5NSA, and 3NSA and one trace gas of NO with sample number of 140 were input into the model for the source apportionment. Note that 4M2,6DNP and 2,4DNP were not included in the model simulation, because 4M2,6DNP was below detection limit in the winter of 2019 and the concentration of 2,4DNP was too low during the sampling periods. Three to six factors were tested by minimizing the objective function Q-value based on the weighted least square. Each simulation was randomly run for 30 times. The optimal number of factors was selected according to several criteria, including the residual distribution, resulting Q values, and a reasonable explanation of source. Almost all scaled residuals were between -3σ and +3σ. The solution with three factors did not distinguish the source factors of secondary formation and vehicle exhaust. The solutions with five or six factors, however, presented two similar source factors characterized by high levels of NO. Therefore, the four-factor solution was finally chosen in this study.

2.5. Spatial concentration weighted trajectory analysis

The spatial concentration weighted trajectory (SCWT) analysis was conducted to compute the weighed mass concentrations of NACs for a single grid passed through by all trajectories, to understand the local and transmission region sources. The traditional concentration weighted trajectory (CWT) method can trace the source regions with frequent trajectories and high levels of air pollutants. However, the uncertainty caused by horizontal and vertical differences in pollutant concentrations is not well taken into account, which will lead to overestimation in clean remote and marine areas. Therefore, in this study the modified SCWT analysis was established and deployed by adding extra horizontal and vertical coefficients (see Eq. (2)). Specifically, the horizontal coefficients were estimated by the normalized gridding surface PM$_{2.5}$ concentrations from the MODIS, MISR, and sea WIFS Aerosol Optical Depth (AOD), which is available from the Socioeconomic Data and Applications Center (https://sedac.ciesin.columbia.edu/data/set/sdei-global-annual-gwr-pm2-5-modis-misr-seawifs-aod-v4-gl-03, last access: 25 June 2022). The vertical coefficients were estimated by the normalized vertically layered PM$_{2.5}$ concentrations in winter based on lidar system from January 2017 to December 2019 from a previous study (Ma et al., 2021).

The 72-hr backward trajectories at the height of 100 m above ground level were calculated by using MeteoInfo software. To boost the reliability of SCWT analysis, all trajectories were calculated at three-hour intervals and the same concentrations were assumed for every half day. The back-trajectory was simulated at 02:00, 05:00, 08:00, and 11:00 UTC (corresponding to 10:00, 13:00, 16:00, and 19:00 local time) for daytime samples, and at 14:00, 17:00, 20:00, and 23:00 UTC (22:00, 01:00, 04:00, and 07:00 local time) for nighttime samples. The meteorological data was provided by the National Centers for Environmental Prediction (ftp://arlftp.arlhq.noaa.gov/pub/archives/, last access: 12 January 2022). The weighed concen-

Table 1 – Average concentrations of individual and total nitro-aromatic compounds, PM$_{2.5}$, and trace gases in coastal Qingdao in the winter of 2018 and 2019 (ng/m^3 except OC and PM$_{2.5}$ in μg/m^3 and NO, NO$_2$, SO$_2$, O$_3$ in ppbv).

Species	Concentrations	
	Winter of 2018 (n= 56)	Winter of 2019 (n = 84)
4NP	36.71 ± 24.72	8.83 ± 5.93
3M4NP	16.46 ± 14.78	3.35 ± 2.75
2M4NP	12.63 ± 10.46	3.43 ± 2.43
2,6DM4NP	8.69 ± 6.26	2.11 ± 1.63
4NC	16.0 ± 14.25	3.99 ± 4.90
4M5NC	4.61 ± 4.64	1.67 ± 2.24
3M6NC	25.51 ± 23.98	2.04 ± 2.98
5NSA	1.05 ± 0.89	0.79 ± 0.80
3NSA	2.16 ± 2.08	1.38 ± 1.19
2,4DNP	0.80 ± 0.91	0.11 ± 0.11
4M2,6DNP	0.40 ± 0.20	/
Total NACs	125.0 ± 89.5	27.7 ± 21.1
OC	25.0 ± 13.5	7.4 ± 5.4
PM$_{2.5}$	128.9 ± 74.9	59.1 ± 47.4
NO	2.8 ± 3.4	3.5 ± 2.8
NO$_2$	21.2 ± 11.6	14.9 ± 7.4
SO$_2$	4.9 ± 2.9	3.1 ± 1.2
O$_3$	25.3 ± 12.6	19.1 ± 9.0

tration of NACs were calculated as follows:

$$C_{ij} = C_0 \times \frac{H_j \times S_j}{\sum_1^{72} H_j \times S_j} \qquad (2)$$

where, i is the trajectory number and j is the trajectory point number. C_{ij} represents the concentration contributed by the trajectory point j on trajectory i, and C_0 is the measured concentration corresponding to the arrival of trajectory i. H_j and S_j are the vertical coefficient and the horizontal coefficient for the trajectory point j, respectively.

In this study, the region of northern China (N 30°∼73°, E 70°∼136°) where trajectories passed over were divided into grid cells with a resolution of 0.25° × 0.25°. Each grid cell was given a weighted concentration value via accumulating the sample concentrations contributed by relevant trajectories passing through the corresponding grid cell.

3. Results and discussion

3.1. Concentration levels and chemical composition

The average concentrations of individual and total nitro-aromatic compounds, PM$_{2.5}$, and trace gases measured in coastal Qingdao in winter are presented in Table 1. In the winter of 2018, the average concentrations of individual NACs in PM$_{2.5}$ ranged from 0.40 ± 0.20 to 36.71 ± 24.72 ng/m^3 (mean ± standard deviation), with the average total concentration of 125.0 ± 89.5 ng m^{-3}. While in the winter of 2019, the concentrations of NACs were relatively low, with the average concentrations of individual NACs ranging from below detection limit to 8.83 ± 5.93 ng/m^3 and the average total concen-
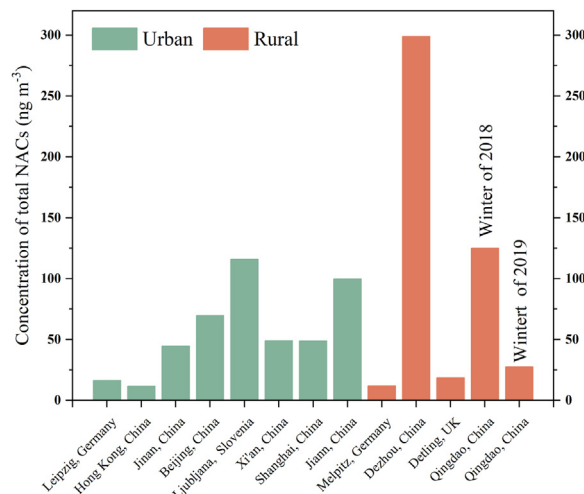

Fig. 2 – Comparison in the total concentrations of NACs in fine particles in coastal Qingdao in this study and those in other locations in cold season from previous studies.

tration of 27.7 ± 21.1 ng/m^3. Meanwhile, the average contents of organic carbon in PM$_{2.5}$ in the winter of 2018 and 2019 were 25.0 ± 13.5 and 7.4 ± 5.4 μg/m^3, respectively, with the value in the winter of 2018 approximately four times of that in 2019, coinciding with the disparities in the NACs concentrations between the two sampling periods. The much higher concentrations of NACs and organic carbon in the winter of 2018 than in 2019 are attributed to the intensive primary emissions and the unfavorable meteorological conditions which are indicated by higher concentrations of PM$_{2.5}$, NO$_2$, SO$_2$, and O$_3$, and more air masses from terrene in the winter of 2018.

Fig. 2 compares the NACs concentrations in fine particles in cold season obtained in the present study in Qingdao and those from previous studies around the world. Generally, the total concentration of NACs in the winter of 2018 in coastal Qingdao was comparable or even higher than those measured in winter in rural and urban sites, apart from rural Dezhou (299 ng/m^3) (Salvador et al., 2021) which was influenced by intense biomass burning and was determined with more nitro-aromatic compounds (16 species). However, it was lower in coastal Qingdao in the winter of 2019 than the previous measured values in urban Xi'an (48.89 ng/m^3) (Yuan et al., 2021), urban Beijing (69.6 ng/m^3) (Wang et al., 2021), urban Shanghai (48.76 ng/m^3) (Cai et al., 2022), urban Jinan (44.54 ng/m^3) (Wang et al., 2018), and urban Ljubljana (116.10 ng/m^3) (Kitanovski et al., 2012), and was similar to those in urban Leipzig (16.28 ng/m^3), rural Melpitz (12.07 ng/m^3) (Teich et al., 2017), and rural Detling (18.72 ng/m^3) (Mohr et al., 2013). Overall, high levels of nitro-aromatic compounds could appear in coastal Qingdao in cold season in some years.

As depicted in Fig. 3, the overall compositions of NACs in coastal Qingdao in the winter of 2018 and 2019 showed no obvious difference, expect that the fraction of 3M6NC was much higher in 2018 (20.4%) than 2019 (7.4%). The higher proportion of 3M6NC observed in the winter of 2018 than 2019 is probably associated with intense biomass burning. Among the mea-
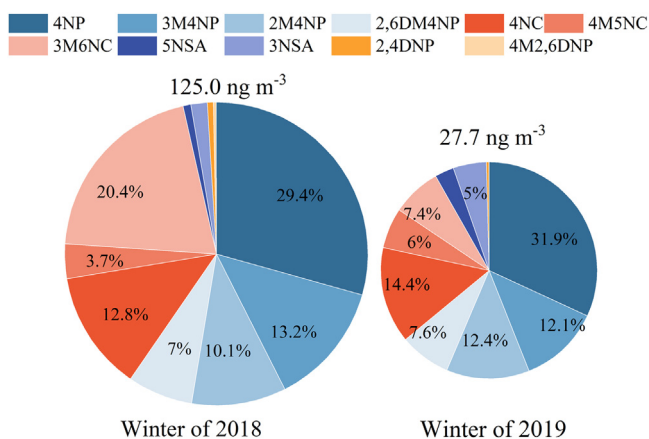
Fig. 3 – Proportions of nitro-aromatic compounds in fine particles in the winter of 2018 and 2019 in coastal Qingdao.

sured species, 4NP and methyl nitrophenols (3M4NP, 2M4NP, and 2,6DM4NP) were found to be the dominant species, which constituted more than half of total NACs. In particular, 4NP made a contribution up to approximately 30%. They were then followed by 4NC and methyl nitrocatechols (4M5NC, and 3M6NC), which accounted for about one-third of total NACs. The contribution of nitrosalicylic acids including 5NSA and 3NSA was moderate, varying between 0.8 and 8%. For 2,4DNP and 4M2,6DNP, their proportions were very small, with average contributions less than 1%. The above composition characteristics are comparable to those studies carried out in winter in northern China such as Jinan (Li et al., 2020a; Wang et al., 2018) and Beijing (Li et al., 2020b, 2020c). In contrary, a large fraction of 2,4DNP was found in summer in Beijing with the average contribution of 23% (Ren et al., 2022), which is possibly related to the enhanced photochemical formation under intensive solar radiation.

3.2. Variation characteristics and influencing factors

Fig. 4 shows the temporal variations of the concentrations of nitro-aromatic compounds, trace gases, as well as meteorological parameters in the winter of 2018 and 2019. Here, the eleven NACs were classified into 4 groups, i.e. nitrophenols (NPs, including 4NP, 3M4NP, 2M4NP, and 2,6DM4NP), nitrocatechols (NCs, including 4NC, 4M5NC, and 3M6NC), nitrosalicylic acids (NSAs, including 5NSA and 3NSA), and dinitrophenols (DNPs, including 2,4DNP and 4M2,6DNP). In the winter of 2018, the total concentration of NACs ranged from 13.6 to 427.4 ng/m^3. The maximum concentration occurred at the night of January 29, 2019, accompanied by high levels of OC and EC and very high humidity (up to 93%), which indicates intensive anthropogenic emissions, facilitated aqueous reactions, and pollutant accumulation in adverse meteorological conditions. Accidentally, a dust event was observed from the night of January 17 to the night of January 19, 2019, as reported by Liang et al. (2020). During the dust event, high levels of NACs appeared along with high concentrations of NO$_x$, SO$_2$, EC, and OC. Particularly, an obvious enhancement of nitrocatechols was observed, with a high average contribution of 55%. The elevated concentrations of NACs (in particular nitrocatechols)

during dust events are partly attributed to the facilitated uptake and enhanced formation on alkaline mineral dusts when the dust plume is mixed with urban plumes. In the winter of 2019, the total concentration of NACs was in the range from 1.41 to 98.1 ng/m^3. The maximum value was monitored at the night of December 21, during which period NO$_x$, SO$_2$, EC, and OC were at very high levels and the humidity was also relatively high. In addition, during the day and night of December 9, high concentrations of NACs (83.8–91.9 ng/m^3) were also observed, accompanied by very high levels of NO$_x$, SO$_2$, EC, and OC.

To understand the influences of anthropogenic emissions and atmospheric conditions on the abundances of fine particulate NACs, we further examine the correlations between NACs and air pollutants and meteorological parameters (see Fig. 5). There are moderately good positive correlations between NACs and SO$_2$, EC, and OC ($r = 0.53$–0.78, $p < 0.01$), indicating that coal burning activities emitted a large amount of NACs in the winter of Qingdao. Moderate positive correlation is also found between NACs and NO$_2$ ($r = 0.61$, $p < 0.01$), suggesting the contributions of traffic exhausts and coal burning plumes and the promotion of NO$_2$ on NAC formation (Wang et al., 2019). In addition, an increasing trend in the concentrations of nitro-aromatic compounds was found at elevated ambient humidity. Relatively high concentrations of NACs appeared under high humidity conditions in the absence of rain, e.g., January 13–14, December 22–24, 2019, mainly due to the pollutant accumulation under unfavorable diffusion conditions and the enhanced formation of fine particle NACs via heterogeneous uptake, gas-liquid/particle partitioning, and/or aqueous reactions. The concentration of NPs exhibits moderate negative correlation with ambient temperature ($r = 0.45$–0.52, $p < 0.01$), which is related to their high vapor pressures and thus they tended to distribute in the gas phase at high temperature conditions (Cecinato et al., 2005). Besides, very strong correlations were found among the same class of nitro-aromatic compounds ($r > 0.9$, $p < 0.01$), demonstrating that they came from same or similar emission sources or formation processes. The good correlations between NPs and NCs were strong ($r = 0.67$–0.8, $p < 0.01$), indicating important contributions from common sources such as coal burning (Lu et al., 2019). However, low correlations were noticed between NSAs and NPs or NCs, because most NSAs came from secondary formation while a large fraction of NPs and NCs were from primary emissions (Cai et al., 2022; Wang et al., 2018).

3.3. Source appointment with receptor model

3.3.1. Source identification
A receptor source apportionment model of EPA PMF 5.0 was employed to identify the major sources of fine particulate nitro-aromatic compounds observed in coastal Qingdao and to quantify their relatively contributions. Finally, four source factors were recognized, including vehicle exhaust, secondary formation, biomass burning, and coal combustion. Fig. 6 depicts the source profiles in the form of concentrations and percentages.

The first factor contributed more than 85% to the total NO, which is recognized as traffic emission based on previ-
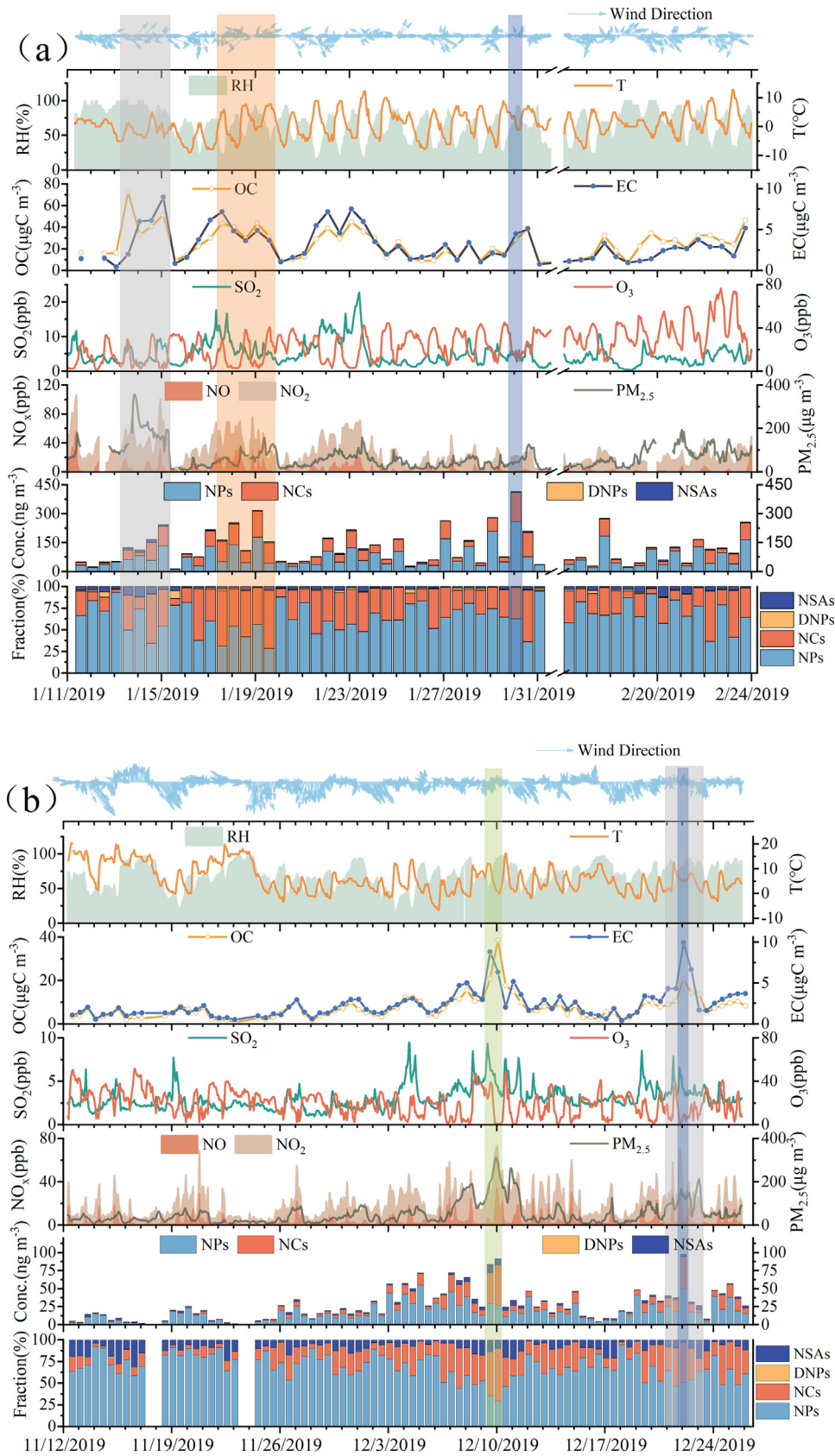
Fig. 4 – Temporal variations of nitro-aromatic compounds, OC, and EC in PM$_{2.5}$, trace pollutants of NO$_x$, O$_3$, SO$_2$, and PM$_{2.5}$, as well as metrological parameters including temperature, relatively humidity, wind speed and direction at coastal Qingdao in the winter of (a) 2018 and (b) 2019. The orange and gray shading refers to dust and high humidity events, respectively. The blue and green shading refers to the samples with maximum and elevated concentrations of total NACs.
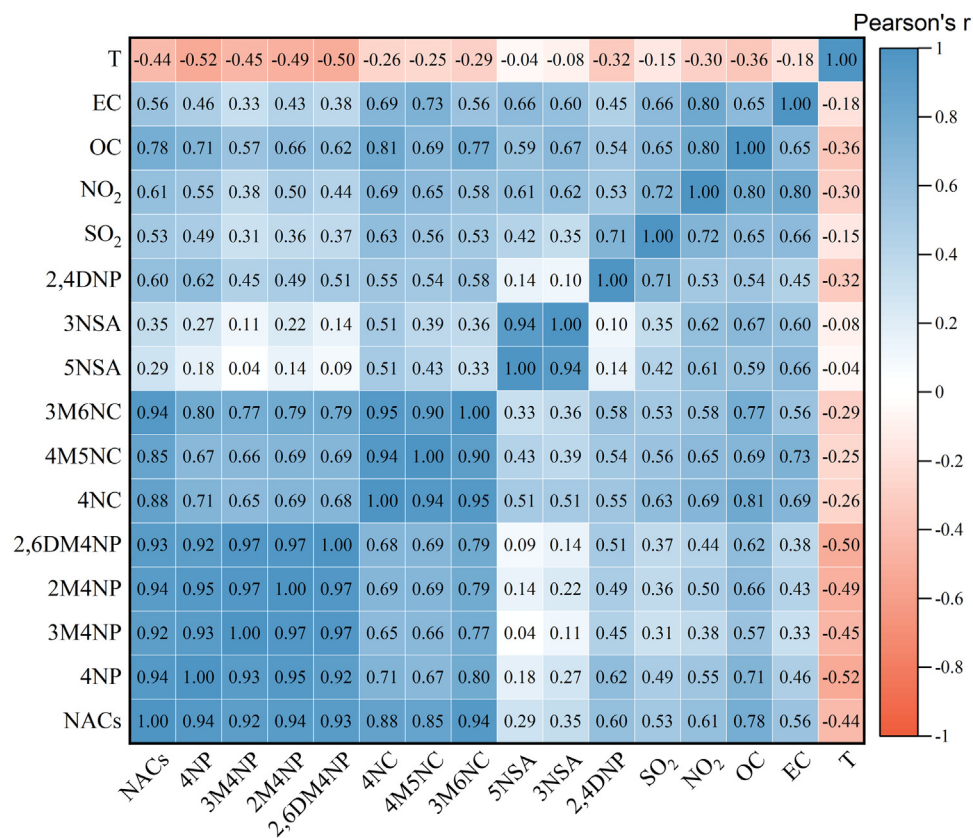
Fig. 5 – The linear correlations among nitro-aromatic compounds and selected gaseous and aerosol pollutants as well as the meteorological parameter including SO_2, NO_2, OC, EC, and temperature.

ous studies (Li et al., 2020a; Ren et al., 2022; Wang et al., 2018). Vehicle exhaust can emit fine particulate NACs with emission factors of 0.68–89.61 µg/km (Lu et al., 2019). This source factor is attributed to the vehicle exhausts in the nearby express way and minor roads as well as ship exhausts in the ocean to the east. The second factor is identified as secondary formation due to the high concentrations and high contributions of 5NSA and 3NSA. It has been confirmed that NSAs are mainly derived from secondary production from previous field and laboratory studies (Andreozzi et al., 2006; Wang et al., 2018; Yuan et al., 2021). The secondary formation of NACs can occur in both gas and aqueous phases and the gas-phase NACs are readily to partly partition into particles due to the semi-volatile property (Chen et al., 2021; Vione et al., 2005). In the third factor, 4-nitrocatechol and methyl-nitrocatechols were most abundant and were characterized by very high contributions. Methyl-nitrocatechol had been identified as the markers for biomass burning plumes with emission factors of 0.75–11.1 mg/kg (Iinuma et al., 2010; Wang et al., 2017). Hence, this source factor is allocated as biomass burning and is caused by the biomass burning activities in nearby villages in winter for heating, cooking, and waste treating purposes. The fourth factor, featuring with high concentrations and high contributions of 4NP, 3M4NP, 2M4NP, and 2,6DM4NP, is considered as coal combustion. This factor profile is very similar to the profile derived in our previous study in urban Jinan (Li et al., 2020a). In that study, coal combustion served as an important con-

tributor of fine particulate NACs especially in cold season and was responsible for the elevated levels of NACs in urban Jinan. The emission factors of fine particulate NACs from residential coal combustion were estimated in the range of 0.2–10.1 mg/kg (Lu et al., 2019b). This source factor is ascribed to the large coal consumption for industrial production, domestic heating, and daily cooking in the adjacent urban and rural areas.

3.3.2.   Source contributions

The contributions of each source to fine particulate NACs are presented in Fig. 7. As shown, coal combustion contributed approximately 80% to 4NP, 3M4NP, 2M4NP, and 2, 6DM4NP and close to 5% to 4NC, 4M5NC, 5NSA, and 3NSA. Biomass burning contributed more than 65% for 4NC, 4M5NC, and 3M6NC and about 5% for 4NP, 3M4NP, and 2,6DM4NP. It is surprising that the above combustion activities contributed more than two thirds to total NACs, 4NP, 3M4NP, 2M4NP, 2,6DM4NP, 4NC, 4M5NC, and 3M6NC. The dominance of solid fuel combustion is mainly attributed to the extensive use of coal and wood for domestic heating and cooking and industrial purpose in nearby rural and urban areas in cold season. In addition, traffic emission contributed more than 20% to 4NC, 4M5NC, 5NSA, and 3NSA and about 5% to total NACs, 2M4NP, and 2,6DM4NP. Secondary formation contributed about 65% to both 5NSA and 3NSA, close to 15% to total NACs, 4NP, and 2M4NP, and approximate 5% for 3M4NP, 2,6DM4NP, and 4NC.
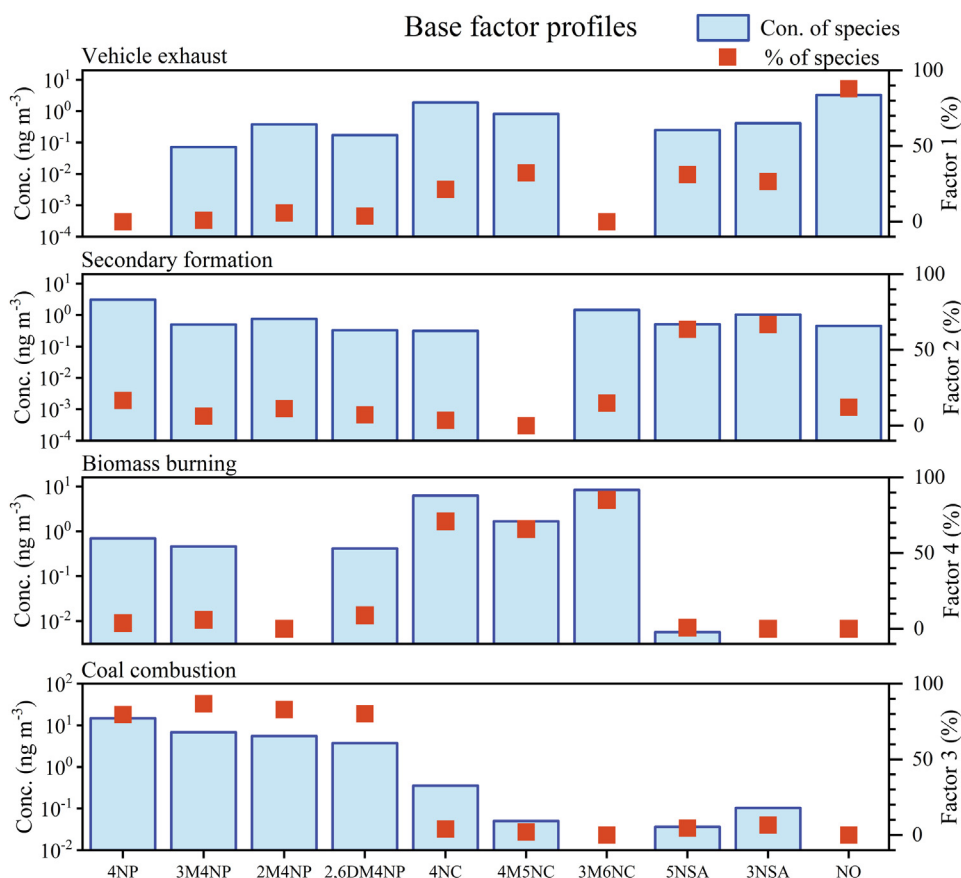
Fig. 6 – Source profiles of fine particulate nitro-aromatic compounds and NO derived by PMF model in coastal Qingdao in winter.
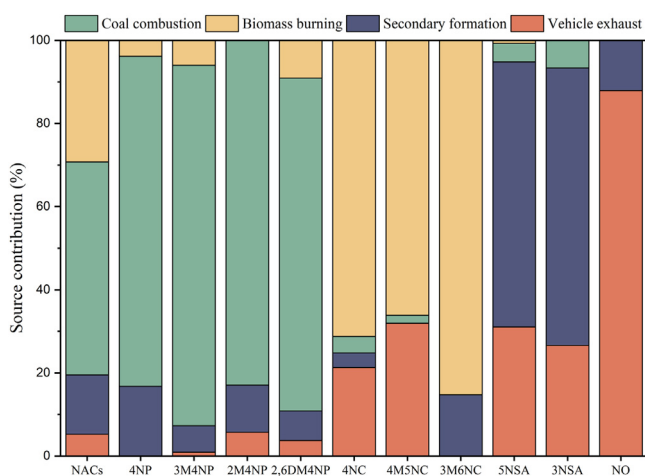

Fig. 7 – Average contributions of four source factors to the concentrations of fine particulate nitro-aromatic compounds in coastal Qingdao in winter.

In comparison with secondary formation, the total contribution of primary emission sources (constituting 85%) is more important during the measurement periods in winter in coastal Qingdao. The result that fine particulate NACs mainly came from primary emissions in coastal areas in this study is consistent to other studies on $PM_{2.5}$-bound NACs conducting in urban areas in northern China in the wintertime (Wang et al., 2018; Li et al., 2020a), while is different from those conducted in the summertime (Ren et al., 2022; Wang et al., 2018; Yuan et al., 2021). Nevertheless, in suburban Nanjing in southern China, combustion sources made much lower contribution (<10%) to NACs in foggy days during winter (Gu et al., 2022) than that in the present study, mainly owing to the much less residential heating activities.

With examination of the specific source contributions to total NACs in the winter of 2018 and 2019, it is found that the contributions of coal combustion are comparable, approximately 50%. However, the contribution of biomass burning in the winter of 2018 (35%) was higher than those in the winter of 2019 (12%). The vehicle exhaust and secondary formation contributed 2% and 11% to NACs in the winter of 2018 and 14% and 24% in the winter of 2019. The higher concentration of NACs in the winter of 2018 than 2019 is possibly related to the stronger contribution from biomass burning source in the winter of 2018.

3.4. *Potential source regions recognized by SCWT analysis*

To further understand the spatial distribution of the primary sources for fine particulate nitro-aromatic compounds in coastal Qingdao in winter, SCWT analysis was applied to in-
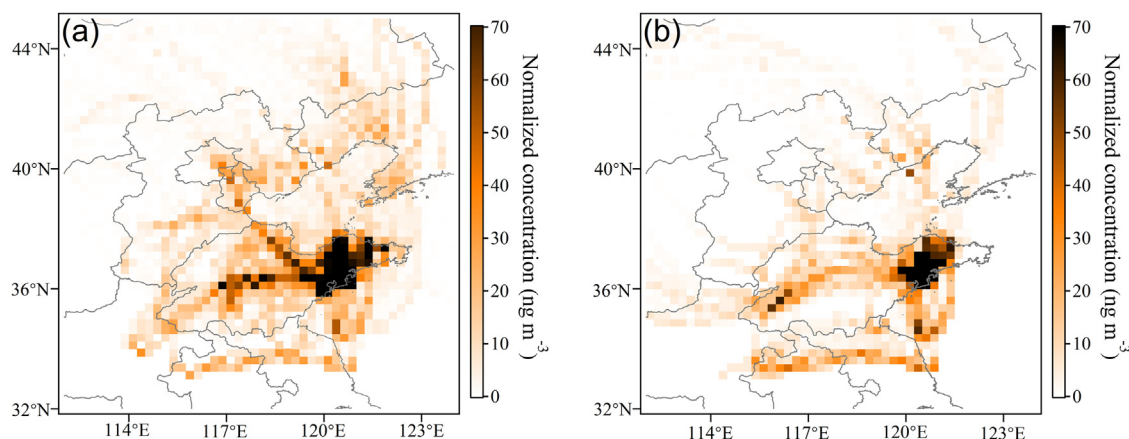
Fig. 8 – Potential source regions derived from the spatial concentration weighted trajectory analysis for PM$_{2.5}$-bound nitro-aromatic compounds in coastal Qingdao in winter for (a) coal combustion source and (b) biomass burning source.

vestigate the potential source regions. In this study, only the samples dominated by primary sources, *i.e.* the contribution of coal combustion large than 50% or that of biomass burning more than 40% based on the PMF results, were selected for further SCWT analysis. Fig. 8 presents the estimated potential source areas. As shown, the coal combustion sources mainly came from Shandong peninsula and small parts in the north and west of Shandong Province. The biomass burning-related sources are located in local Qingdao and a few rural areas to the west of Qingdao. The large population, intensive industries, and huge consumption of solid fuels (in particular coal) in Shandong province make it an important contributor to the atmospheric NACs in adjacent regions. As reported in previous studies, the air masses influenced by coal and biomass combustion mostly from northern heating areas were major sources of fine particulate NACs in Shanghai during the wintertime (Cai et al., 2022). In addition, the gas-phase NACs dominated by biomass burning in Beijing in winter primarily originated from Tianjin city of Shandong province (Song et al., 2021a). The above results and evidences demonstrate the important role of regional transport of air masses from Shandong province playing in the high levels of NACs.

Overall, the potential source regions of fine particulate NACs in coastal Qingdao in winter mainly distributed in the local Shandong Province, in particular the eastern Shandong. With consideration the large contributions from coal combustion and biomass burning to the high levels of NACs, emission control via strategies of clean combustion and replacement with clean energy in Shandong Province is urgently needed for reducing the concentrations of fine particulate NACs in Qingdao.

Conclusions

In this study, nitro-aromatic compounds in fine particles in coastal Qingdao in winter were measured by using UHPLC-MS. The average concentrations of total NACs in the winter of 2018 and 2019 were 125.0 ± 89.5 and 27.7 ± 21.1 ng/m^3, re-

spectively. Nitrophenol, nitrocatechol, and the methyl substitutes were the dominant species among the detected components, with their total contribution exceeding 90%. The concentrations of NACs exhibited good correlations with SO$_2$, NO$_2$, EC, and OC, indicating the strong influences from primary emissions. NACs tended to be in high levels in the conditions of high humidity on foggy days, which is attributed to the pollutant accumulation and the enhanced secondary formation. According to the PMF derived results, four source factors were primarily responsible for the observed fine particulate NACs in coastal Qingdao in winter. Solid fuel combustion sources (coal combustion and biomass burning) contributed the largest fraction, with the total contribution up to 80%, followed by secondary formation (15%) and vehicle exhaust (5%). The SCWT analysis showed that the potential source regions were mainly located in Shandong Province (especially the eastern part). Overall, this work highlights the dominant contributions of coal combustion and biomass burning from local and surrounding areas to the atmospheric fine particulate NACs in coastal Qingdao in winter. It is urgently required to reduce the emissions from coal combustion and biomass to address the problem of high levels of NACs in cold season.

Declaration of Competing Interest

The authors declare that they have no known competing financial interests or personal relationships that could have appeared to influence the work reported in this paper.

Acknowledgments

REFERENCES

Agency for Toxic Substances and Disease Registry: https://www.atsdr.cdc.gov/phs/phs.asp?id=878&tid=172, 2015 (last access: 27 January 2022).

Andreozzi, R., Canterino, M., Caprio, V., Di Somma, I., Sanchirico, R., 2006. Salicylic acid nitration by means of nitric acid/acetic acid system: chemical and kinetic characterization. Org. Process Res. Dev. 10, 1199–1204. doi:10.1021/op060148o.

Bejan, I., Abd El Aal, Y., Barnes, I., Benter, T., Bohn, B., Wiesen, P., Kleffmann, J., 2006. The photolysis of ortho-nitrophenols: a new gas phase source of HONO. Phys. Chem. Chem. Phys. 8, 2028–2035. doi:10.1039/b516590c.

Bidleman, T.F., 1988. Wet and dry deposition of organic compounds are controlled by their vapor-particle partitioning. Environ. Sci. Technol. 22, 361–367. doi:10.1021/es00169a002.

Brown, S.G., Eberly, S., Paatero, P., Norris, G.A., 2015. Methods for estimating uncertainty in PMF solutions: examples with ambient air and water quality data and guidance on reporting PMF results. Sci. Total Environ. 518–519, 626–635. doi:10.1016/j.scitotenv.2015.01.022.

Cai, D., Wang, X., George, C., Cheng, T., Herrmann, H., Li, X., et al., 2022. Formation of secondary nitroaromatic compounds in polluted urban environments. J. Geophys. Res. Atmos. 127. doi:10.1029/2021JD036167.

Cecinato, A., Di Palo, V., Pomata, D., Tomasi Scianò, M.C., Possanzini, M., 2005. Measurement of phase-distributed nitrophenols in Rome ambient air. Chemosphere 59, 679–683. doi:10.1016/j.chemosphere.2004.10.045.

Chen, Y., Zheng, P., Wang, Z., Pu, W., Tan, Y., Yu, C., et al., 2021. Secondary formation and impacts of gaseous nitro-phenolic compounds in the continental outflow observed at a background site in South China. Environ. Sci. Technol. 6933–6943. doi:10.1021/acs.est.1c04596.

Cheng, I., Zhang, L., Blanchard, P., Dalziel, J., Tordon, R., 2013. Concentration-weighted trajectory approach to identifying potential sources of speciated atmospheric mercury at an urban coastal site in Nova Scotia, Canada. Atmos. Chem. Phys. 13, 6031–6048. doi:10.5194/acp-13-6031-2013.

Cheng, S., Zhou, C., Yin, H., Sun, J., Han, K., 2009. OH produced from o-nitrophenol photolysis: a combined experimental and theoretical investigation. J. Chem. Phys. 130, 234311. doi:10.1063/1.3152635.

Chow, K.S., Huang, X.H.H., Yu, J., 2015. Quantification of nitroaromatic compounds in atmospheric fine particulate matter in Hong Kong over 3 years: field measurement evidence for secondary formation derived from biomass burning emissions. Environ. Chem. 13, 665–673. doi:10.1071/EN15174.

Delhomme, O., Morville, S., Millet, M., 2010. Seasonal and diurnal variations of atmospheric concentrations of phenols and nitrophenols measured in the Strasbourg area, France. Atmos. Pollut. Res. 1, 16–22. doi:10.5094/APR.2010.003.

Feng, X., Tian, Y., Xue, Q., Song, D., Huang, F., Feng, Y., 2021. Measurement report: spatiotemporal and policy-related variations of PM$_{2.5}$ composition and sources during 2015–2019 at multiple sites in a Chinese megacity. Atmos. Chem. Phys. 21, 16219–16235. doi:10.5194/acp-21-16219-2021.

Gu, C., Cui, S., Ge, X., Wang, Z., Chen, M., Qian, Z., et al., 2022. Chemical composition, sources and optical properties of nitrated aromatic compounds in fine particulate matter during winter foggy days in Nanjing, China. Environ. Res. 212, 113255. doi:10.1016/j.envres.2022.113255.

Harrison, M.A.J., Barra, S., Borghesi, D., Vione, D., Arsene, C., Iulian Olariu, R., 2005. Nitrated phenols in the atmosphere: a review. Atmos. Environ. 39, 231–248. doi:10.1016/j.atmosenv.2004.09.044.

Hoffmann, D., Iinuma, Y., Herrmann, H., 2007. Development of a method for fast analysis of phenolic molecular markers in biomass burning particles using high performance liquid chromatography/atmospheric pressure chemical ionisation mass spectrometry. J. Chromatogr. A 1143, 168–175. doi:10.1016/j.chroma.2007.01.035.

Iinuma, Y., Böge, O., Gräfe, R., Herrmann, H., 2010. Methyl-nitrocatechols: atmospheric tracer compounds for biomass burning secondary organic aerosols. Environ. Sci. Technol. 44, 8453–8459. doi:10.1021/es102938a.

Kahnt, A., Behrouzi, S., Vermeylen, R., Safi Shalamzari, M., Vercauteren, J., Roekens, E., et al., 2013. One-year study of nitro-organic compounds and their relation to wood burning in PM$_{10}$ aerosol from a rural site in Belgium. Atmos. Environ. 81, 561–568. doi:10.1016/j.atmosenv.2013.09.041.

Kitanovski, Z., Grgić, I., Vermeylen, R., Claeys, M., Maenhaut, W., 2012. Liquid chromatography tandem mass spectrometry method for characterization of monoaromatic nitro-compounds in atmospheric particulate matter. J. Chromatogr. A 1268, 35–43. doi:10.1016/j.chroma.2012.10.021.

Kovacic, P., Somanathan, R., 2014. Nitroaromatic compounds: environmental toxicity, carcinogenicity, mutagenicity, therapy and mechanism: nitro aromatic pollutants. J. Appl. Toxicol. 34, 810–824. doi:10.1002/jat.2980.

Li, M., Wang, X., Lu, C., Li, R., Zhang, J., Dong, S., Yang, L., Xue, L., Chen, J., Wang, W., 2020a. Nitrated phenols and the phenolic precursors in the atmosphere in urban Jinan, China. Sci. Total Environ. 714, 136760. doi:10.1016/j.scitotenv.2020.136760.

Li, Q., Gong, D., Wang, H., Wang, Y., Han, S., Wu, G., et al., 2022. Rapid increase in atmospheric glyoxal and methylglyoxal concentrations in Lhasa, Tibetan Plateau: potential sources and implications. Sci. Total Environ. 824, 153782. doi:10.1016/j.scitotenv.2022.153782.

Li, X., Wang, Y., Hu, M., Tan, T., Li, M., Wu, Z., Chen, S., Tang, X., 2020b. Characterizing chemical composition and light absorption of nitroaromatic compounds in the winter of Beijing. Atmos. Environ. 237, 117712. doi:10.1016/j.atmosenv.2020.117712.

Li, X., Yang, Y., Liu, S., Zhao, Q., Wang, G., Wang, Y., 2020c. Light absorption properties of brown carbon (BrC) in autumn and winter in Beijing: composition, formation and contribution of nitrated aromatic compounds. Atmos. Environ. 223, 117289. doi:10.1016/j.atmosenv.2020.117289.

Liang, Y., Wang, X., Dong, S., Liu, Z., Mu, J., Lu, C., et al., 2020. Size distributions of nitrated phenols in winter at a coastal site in north China and the impacts from primary sources and secondary formation. Chemosphere 250, 126256. doi:10.1016/j.chemosphere.2020.126256.

Liu, Z., Li, M., Wang, X., Liang, Y., Jiang, Y., Chen, J., et al., 2022. Large contributions of anthropogenic sources to amines in fine particles at a coastal area in northern China in winter. Sci. Total Environ. 839, 156281. doi:10.1016/j.scitotenv.2022.156281.

Lu, C., Wang, X., Dong, S., Zhang, J., Li, J., Zhao, Y., Liang, Y., Xue, L., Xie, H., Zhang, Q., Wang, W., 2019a. Emissions of fine particulate nitrated phenols from various on-road vehicles in China. Environ. Res. 179, 108709. doi:10.1016/j.envres.2019.108709.

Lu, C., Wang, X., Li, R., Gu, R., Zhang, Y., Li, W., Gao, R., Chen, B., Xue, L., Wang, W., 2019b. Emissions of fine particulate nitrated phenols from residential coal combustion in China. Atmos. Environ. 203, 10–17. doi:10.1016/j.atmosenv.2019.01.047.

Lu, C., Wang, X., Zhang, J., Liu, Z., Liang, Y., Dong, S., et al., 2021. Substantial emissions of nitrated aromatic compounds in the

particle and gas phases in the waste gases from eight industries. Environ. Pollut. 283, 117132. doi:10.1016/j.envpol.2021.117132.

Luo, L., Bai, X., Liu, S., Wu, B., Liu, W., Lv, Y., et al., 2022. Fine particulate matter ($PM_{2.5}/PM_{1.0}$) in Beijing, China: variations and chemical compositions as well as sources. J. Environ. Sci. 121, 187–198. doi:10.1016/j.jes.2021.12.014.

Lüttke, J., Scheer, V., Levsen, K., Wünsch, G., Neil Cape, J., Hargreaves, K.J., et al., 1997. Occurrence and formation of nitrated phenols in and out of cloud. Atmos. Environ. 31, 2637–2648. doi:10.1016/S1352-2310(96)00229-4.

Ma, Y., Zhu, Y., Liu, B., Li, H., Jin, S., Zhang, Y., Fan, R., Gong, W., 2021. Estimation of the vertical distribution of particle matter ($PM_{2.5}$) concentration and its transportflux from lidar measurements based on machine learning algorithms. Atmos. Chem. Phys. 21, 17003–17016. doi:10.5194/acp-21-17003-2021.

Mohr, C., Lopez-Hilfiker, F.D., Zotter, P., Prévôt, A.S.H., Xu, L., Ng, N.L., et al., 2013. Contribution of nitrated phenols to wood burning brown carbon light absorption in Detling, United Kingdom during winter time. Environ. Sci. Technol. 47, 6316–6324. doi:10.1021/es400683v.

Morville, S., Scheyer, A., Mirabel, P., Millet, M., 2006. Spatial and geographical variations of urban, suburban and rural atmospheric concentrations of phenols and nitrophenols. Environ. Sci. Pollut. Res. 13, 83–89. doi:10.1065/espr2005.06.264.

Reizer, M., Calzolai, G., Maciejewska, K., Orza, J.A.G., Carraresi, L., Lucarelli, F., et al., 2021. Measurement report: receptor modeling for source identification of urban fine and coarse particulate matter using hourly elemental composition. Atmos. Chem. Phys. 21, 14471–14492. doi:10.5194/acp-21-14471-2021.

Ren, Y., Wei, J., Wang, G., Wu, Z., Ji, Y., Li, H., 2022. Evolution of aerosol chemistry in Beijing under strong influence of anthropogenic pollutants: composition, sources, and secondary formation of fine particulate nitrated aromatic compounds. Environ. Res. 204, 111982. doi:10.1016/j.envres.2021.111982.

Salvador, C.M.G., Tang, R., Priestley, M., Li, L., Tsiligiannis, E., Le Breton, M., et al., 2021. Ambient nitro-aromatic compounds – biomass burning versus secondary formation in rural China. Atmos. Chem. Phys. 21, 1389–1406. doi:10.5194/acp-21-1389-2021.

Song, K., Guo, S., Wang, H., Yu, Y., Wang, H., Tang, R., Xia, S., Gong, Y., Wan, Z., Lv, D., Tan, R., Zhu, W., Shen, R., Li, X., Yu, X., Chen, S., Zeng, L., Huang, X., 2021a. Measurement report: online measurement of gas-phase nitrated phenols utilizing a CI-LToF-MS: primary sources and secondary formation. Atmos. Chem. Phys. 21, 7917–7932. doi:10.5194/acp-21-7917-2021.

Song, M., Li, X., Yang, S., Yu, X., Zhou, S., Yang, Y., Chen, S., Dong, H., Liao, K., Chen, Q., Lu, K., Zhang, N., Cao, J., Zeng, L., Zhang, Y., 2021b. Spatiotemporal variation, sources, and secondary transformation potential of volatile organic compounds in Xi'an, China. Atmos. Chem. Phys. 21, 4939–4958. doi:10.5194/acp-21-4939-2021.

Teich, M., van Pinxteren, D., Wang, M., Kecorius, S., Wang, Z., Müller, T., et al., 2017. Contributions of nitrated aromatic compounds to the light absorption of water-soluble and particulate brown carbon in different atmospheric environments in Germany and China. Atmospheric Chem. Phys. 17, 1653–1672. doi:10.5194/acp-17-1653-2017.

Tremp, J., Mattrel, P., Fingler, S., Giger, W., 1993. Phenols and nitrophenols as tropospheric pollutants: emissions from automobile exhausts and phase transfer in the atmosphere. Water. Air. Soil Pollut. 68, 113–123. doi:10.1007/BF00479396.

Vione, D., Maurino, V., Minero, C., Pelizzetti, E., 2005. Aqueous atmospheric chemistry: formation of 2,4-dinitrophenol upon nitration of 2-nitrophenol and 4-nitrophenol in solution. Environ. Sci. Technol. 39, 7921–7931. doi:10.1021/es050824m.

Wang, H., Gao, Y., Wang, S., Wu, X., Liu, Y., Li, X., et al., 2020. Atmospheric processing of nitrophenols and nitrocresols from biomass burning emissions. J. Geophys. Res. Atmos. 125. doi:10.1029/2020JD033401.

Wang, L., Wang, X., Gu, R., Wang, H., Yao, L., Wen, L., et al., 2018. Observations of fine particulate nitrated phenols in four sites in northern China: concentrations, source apportionment, and secondary formation. Atmos. Chem. Phys. 18, 4349–4359. doi:10.5194/acp-18-4349-2018.

Wang, X., Gu, R., Wang, L., Xu, W., Zhang, Y., Chen, B., Li, W., Xue, L., Chen, J., Wang, W., 2017. Emissions of fine particulate nitrated phenols from the burning of five common types of biomass. Environ. Pollut. 230, 405–412. doi:10.1016/j.envpol.2017.06.072.

Wang, Y., Hu, M., Wang, Y., Zheng, J., Shang, D., Yang, Y., et al., 2019. The formation of nitro-aromatic compounds under high NOx and anthropogenic VOC conditions in urban Beijing, China. Atmos. Chem. Phys. 19, 7649–7665. doi:10.5194/acp-19-7649-2019.

Wang, Z., Zhang, J., Zhang, L., Liang, Y., Shi, Q., 2021. Characterization of nitroaromatic compounds in atmospheric particulate matter from Beijing. Atmos. Environ. 246, 118046. doi:10.1016/j.atmosenv.2020.118046.

Wong, Y.K., Liu, K.M., Yeung, C., Leung, K.K.M., Yu, J.Z., 2022. Measurement report: characterization and source apportionment of coarse particulate matter in Hong Kong: Insights into the constituents of unidentified mass and source origins in a coastal city in southern China. Atmos. Chem. Phys. 22, 5017–5031. doi:10.5194/acp-2021-1030.

Xing, L., Fu, T., Cao, J.J., Lee, S.C., Wang, G.H., Ho, K.F., et al., 2013. Seasonal and spatial variability of the OM/OC mass ratios and high regional correlation between oxalic acid and zinc in Chinese urban organic aerosols. Atmos. Chem. Phys. 13, 4307–4318. doi:10.5194/acp-13-4307-2013.

Yang, Z., Tsona, N.T., George, C., Du, L., 2022. Nitrogen-containing compounds enhance light absorption of aromatic-derived brown carbon. Environ. Sci. Technol. 56, 4005–4016. doi:10.1021/acs.est.1c08794.

Yuan, W., Huang, R., Yang, L., Wang, T., Duan, J., Guo, J., et al., 2021. Measurement report: $PM_{2.5}$-bound nitrated aromatic compounds in Xi'an, Northwest China – seasonal variations and contributions to optical properties of brown carbon. Atmos. Chem. Phys. 21, 3685–3697. doi:10.5194/acp-21-3685-2021.

Zhang, X., Lin, Y., Surratt, J.D., Weber, R.J., 2013. Sources, composition and absorption ångström exponent of light-absorbing organic components in aerosol extracts from the Los Angeles basin. Environ. Sci. Technol. 47, 3685–3693. doi:10.1021/es305047b.

Zhang, X., Wang, J., Zhang, K., Shang, X., Aikawa, M., Zhou, G., et al., 2022. Year-round observation of atmospheric inorganic aerosols in urban Beijing: Size distribution, source analysis, and reduction mechanism. J. Environ. Sci. 114, 354–364. doi:10.1016/j.jes.2021.09.014.